

Review

Micromechanical testing of bone trabeculae - potentials and limitations

E. LUCCHINETTI*, D. THOMANN, G. DANUSER

BioMicroMetrics Group, Laboratory for Biomechanics, Swiss Federal Institute of Technology Zurich (ETHZ), Schlieren, Switzerland
 E-mail: lucchinetti@biomech.mat.ethz.ch

The mechanical properties of bone are studied mostly for reasons related to skeletal pathology. However, bone is also very interesting from a material science perspective because it is a natural hierarchical composite material. The mechanical properties of bone depend on both the structural arrangement and the properties of the constituting materials, namely the organic polymer collagen and the inorganic salt apatite. While the mechanical properties of bone samples at the macroscopic scale are measured routinely, mechanical tests on micrometer-sized specimens are still at development stage. In this paper, protocols for measuring the elasticity of cancellous bone trabeculae are reviewed. The published values for the elastic modulus of trabeculae vary between 1 GPa and 15 GPa. Reasons for this broad range of values may be located in the intrinsic difficulties of preparing, handling, and testing inhomogeneous, anisotropic and asymmetric micro-samples. We discuss the major error sources in existing testing procedures and suggest potential strategies to enhance their performance. © 2000 Kluwer Academic Publishers

1. Introduction

Age-related bone fragility represents a significant social and economic problem in the elderly population. Osteoporosis - the medical condition describing increased incidence of fractures in the elderly - is thought to be not only the result of a reduced bone mass but also of an altered *bone quality* [1]. Bone quality – a term yet to be precisely defined – describes the mechanical performance of bone tissue as a material and obviously depends on the mechanical properties of bone. Additionally, bone undergoes constant, adaptational changes in response to local alterations in stress distribution (*Wolff's law* [2]). Therefore, the quantification of bone mechanical properties is important in the diagnosis of age-related bone fragility and for the understanding of bone adaptation to other natural as well as artificial impacts.

Bone is a composite material. The main components are collagen type I and a mineral phase, best defined as poorly crystalline apatite. Clearly, the mechanical properties of bone depend upon the properties of these constituents. However, it is not only the molecular structure and arrangement of the organic and mineral phases, but also the geometric organization inside the composite tissue, which determine the mechanical behavior of bone at the microscopic and macroscopic scales.

In this review we discuss a number of methods used to quantify the mechanical properties of cancellous bone.

We focus on experiments that aim at the mechanical characterization of individual trabeculae. As it shall be seen, trabeculae are the basic micro-structural units forming cancellous bone tissue. Sec. 2 is dedicated to a review of the structural scale hierarchy of bone. We define a length scale in order to assign the various bone structures to one of the levels in this hierarchy. In Sec. 3 we point out analogies and differences between the mechanical properties and related testing methods at the macroscopic and microscopic scale and present the essential findings from macroscopic testing procedures. Sec. 4 describes the state of the art in testing single cancellous bone trabeculae. We pool the results and attempt to classify the reported values in a comparative manner. In Sec. 5 we analyze potential sources of error and derive from it the limitations in significance of published experiments. Finally, we conclude with an attempt to name the most important factors which may contribute to an improvement of the state of the art in single trabecula testing (Sec. 6).

2. Structural hierarchy of bone

Bone is both a composite and hierarchically structured material. Several organizational levels can be identified [3, 4]. Fig. 1 illustrates the hierarchy of bone from the macroscopic level to the nanometer-sized molecular components. Based on the macroscopic appearance

* Author to whom all correspondence should be addressed.

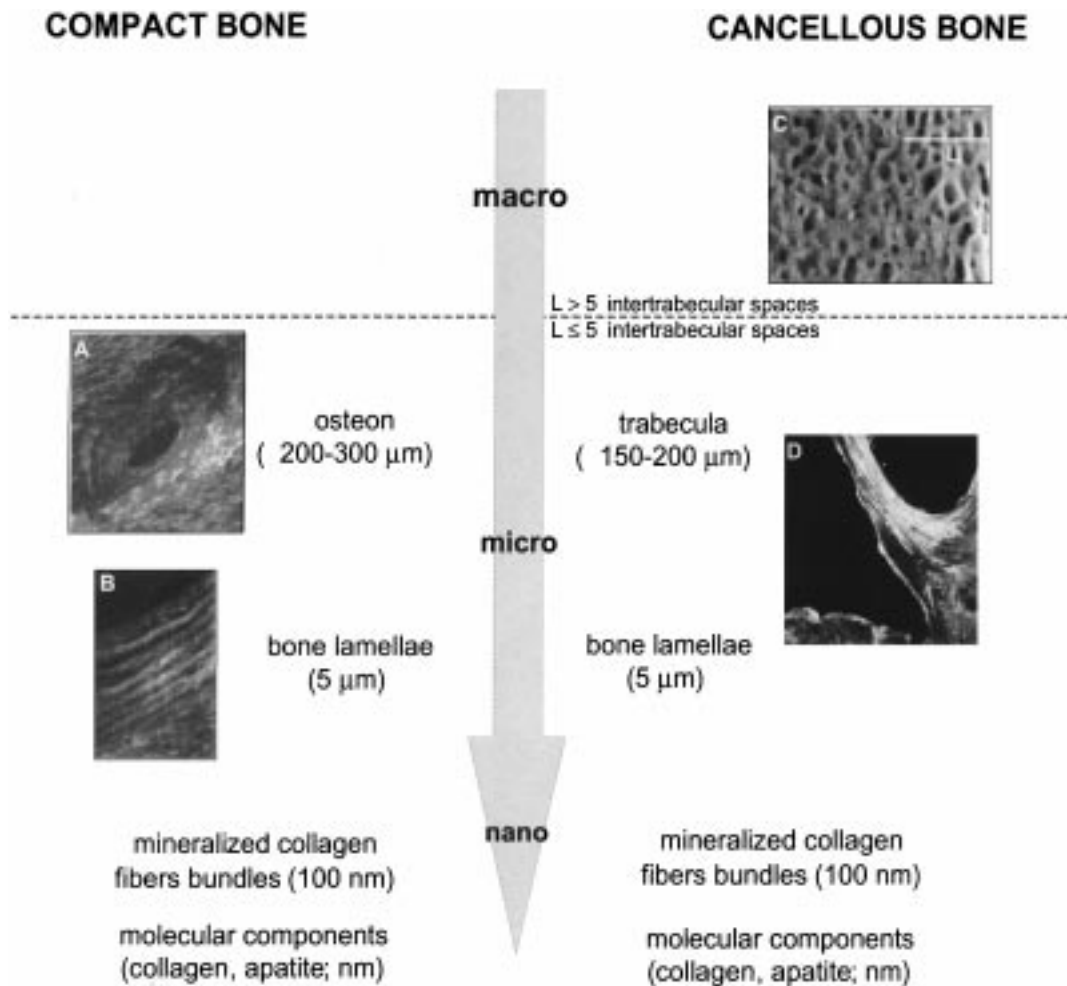


Figure 1 On the macroscopic scale, two types of bone can be distinguished: compact bone and cancellous bone. The basic microstructural unit of compact (haversian) bone is the osteon (panel A). This image of an osteon from human cortical bone was obtained using a scanning electron microscope (Philips, USA) operated at 20 kV (magnification 360×). The concentric lamellar structure at higher magnification (acceleration voltage 20 kV, magnification 2000×) is presented in panel B. Cancellous bone consists of a lattice of trabeculae, as illustrated in panel C. The image has been captured using a CCD camera (Leutron Vision, Switzerland) mounted on a stereo light microscope (STEMI SV 11, Carl Zeiss, Germany) at 8× magnification. At the microscopical level, the basic microstructural unit in cancellous bone is the trabecula (panel D). This image has been obtained using a confocal laser scanning microscope (LSM 510, Carl Zeiss, Germany). The excitation wavelength was 543 nm and a long-pass filter ($\lambda > 550$ nm) has been used to capture the emitted radiation. The objective used was a Plan-Neofluar 20× with a numerical aperture of 0.5. The tissue clearly exhibits autofluorescence. Also, the lamellar structure can be observed using this contrast modus.

and the anatomical location, two types of bone are distinguished: cortical bone and cancellous bone. Cortical bone is the dense tissue that primarily forms the outer shell of all bones. Cortical bone tissue consists of osteons, which are hollow cylindrical structures with a diameter of 200–300 μm surrounding a blood vessel (Haversian canal). The osteons are interfaced from the interstitial bone tissue by a thin layer (1–5 μm thick) of apparently amorphous substance called cement line. Osteons appear as layered structures made of concentric lamellae, each approximately 5 μm thick. Lamellae are compounds of mineralized collagen. Inside the lamellar structure, osteocytes (the bone cells) reside in ellipsoidal cavities with a volume of approximately $15 \times 10 \times 7 \mu\text{m}^3$ [5]. They are referred as lacunae.

In contrast to cortical bone, cancellous bone is highly porous at the macroscopic level. It is primarily found in the terminal regions of long bones and in vertebral bodies. The macroscopic structure of cancellous bone consists of a complex meshwork of interconnected rods and plates called trabeculae. Trabeculae are the basic structural units in cancellous bone and consist of miner-

alized collagen layers, analogous to the osteon forming lamellae in cortical bone tissue. The lamellae in cancellous bone tissue are preferentially aligned with the long axis of the trabeculae. Cement lines are also observed in trabecular bone separating groups of lamellae originating from different periods of bone generation and remodeling. These groups of lamellae are called trabecular packets. The thickness of the trabeculae varies between 100 μm and 300 μm. The inter-trabecular distance ranges from 0.5 mm to 1.5 mm or more. Most morphometric studies on cancellous bone have focused on the characteristics of cancellous bone architecture, including trabecular thickness, spacing, and orientation [6, 7]. However, to our knowledge the morphology of sub-trabecular structures has been systematically addressed in one study [8].

The lamellae in both compact and cancellous bone consist of mineralized collagen fibrils. The extremely small plate-shaped apatite crystals, a few hundreds angstroms long and wide and 20 to 30 angstroms thick, are arranged in an ordered manner within the collagen framework. At the nanoscopic scale the underlying

composite material is supposed to be equal for cortical and cancellous bone. Provided that the mechanisms by which bone is resorbed and laid down are very similar in cortical and cancellous bone, cortical and cancellous bone lamellae might have similar mechanical properties. This has already been postulated by Wolff [2] in 1892. Actually, Wolff went a step further and argued that the two types of bone have identical properties at the microscopic scale. He underpinned his statement with the observation that there is a smooth transition between cancellous bone and cortical bone when moving from the center to the periphery of a whole piece of bone. With regard to the large variability in the published results of micro-testing, Wolff's hypothesis remains very speculative and still awaits a confirmation based on rigorous theoretical and experimental investigations.

3. The mechanical properties of cancellous bone

Both cortical and cancellous bone are viscoelastic materials. However, the mechanical properties depend weakly on strain rate [9]. In the following, we will consider cancellous bone as an elastic material.

A linear elastic material subjected to uniaxial stress can be described by its stiffness or Young's modulus E . E relates changes in stress and strain in a linear fashion (Hooke's law: $\sigma = E * \epsilon$). In the general form, Hooke's law is written as the stress tensor being the product between the stiffness matrix and the strain tensor [10]:

$$T_{ij} = C_{ijkl} * e_{km}$$

The matrix C_{ijkl} denotes the fourth rank tensor of the elastic coefficients, whereas T_{ij} and e_{km} are the second rank cartesian stress and strain tensors. The degrees of freedom of the stiffness matrix, i.e. the number of independent matrix elements, depends on the type of material symmetries in the sample [11]. Measurements of the mechanical properties are generally confined to specific directions, not aiming at the determination of the entire stiffness matrix in its general form.

The mechanical properties of trabecular bone are usually referred to as the mechanical properties of a macroscopic piece of cancellous bone. Cancellous bone shows a large variability in terms of porosity and structural orientation. Some of these variations are associated with regional adaptation to external load exposure, according to *Wolff's law* [2], others are effected by biochemical processes such as bone resorption and deposition. Samples from different regions and of different bone age have a different trabecular architecture. These architectural parameters have an essential impact on the measured mechanical property of cancellous bone samples. It has been shown that cancellous bone exhibits highly anisotropic behavior at the macroscopic scale [12]. The actual material composition appears to have only a secondary influence compared to the impact of the structural arrangement.

On the scale of single trabeculae, the molecular structure of the organic and inorganic components and their interfaces as well as the presence of lacunae (i.e. defects

from a materials science point of view) have a much larger impact on the mechanical properties. It remains to show how much the lamellar architecture influences the behavior of isolated trabeculae. In analogy to observations made on the macroscopic scale one can expect that the inhomogeneous arrangement of lamellae will cause anisotropy also in the mechanical properties of trabeculae. A further question to be addressed concerns the degree of regional and temporal variation in the lamellar structure induced by adaptive processes.

From these comments it is evident that a mechanical testing of macroscopic bone specimens does not necessarily reflect the properties of microscopic samples. In order to understand the material *bone* it is necessary to determine at the different hierarchical levels. Constitutive laws have to be formulated to cross-link the various hierarchical levels. Such multi-scale integration allows to aim for a complete understanding of the interaction between the structural levels of the composite and their impact on the overall mechanical performance of the material bone.

In the following, we distinguish between the scales by referring to mechanical properties of *cancellous bone* as those measured on the *macroscopic level* and to the properties of *trabecular bone material* as those measured on the *microscopic level*. Harrigan *et al.* showed that cancellous bone volumes having a side length of 5 inter-trabecular spaces (ITS) and more can be modeled in good approximation as a continuum [13]. Bone specimens satisfying Harrigan's conditions will be termed as macrosamples, whereas cancellous bone volumes with a side length smaller than 5 ITS will be called microsamples (cf. Fig. 1).

3.1. Direct measurement of mechanical properties in cancellous bone samples

Over the years, many researchers have measured elastic properties of cancellous bone samples. The results indicate that the stiffness of cancellous bone varies over a wide range of values and it is dependent on the anatomical location [12].

It is generally assumed that three planes of symmetry exist. Hence, cancellous bone is an orthotropic material [14], with an elastic behavior being fully described by nine constants. The most common mechanical test performed is the compression test. A cubic specimen is compressed between two steel plates and the applied force and the resulting axial deformation are recorded. The test can be repeated for the other two spatial directions, which yields an estimate of three independent elastic moduli. The determination of both the Poisson ratios and the shear moduli requires a more sophisticated experimental setup.

As an alternative to compression test, mechanical behavior can be derived from ultrasound measurements. Ultrasound is a small amplitude, high strain rate mechanical test that has been successfully used in bone research [15, 16]. Ultrasound has the advantage that all of the nine orthotropic elastic constants can be determined. Longitudinal velocities v_i of waves propagating in the i -direction, and shear wave velocities c_{ij} propagating in the i -direction with particle motion in

the j -direction are related to the longitudinal and shear moduli by $E_i = \rho * v_i^2$ and $G_{ij} = \rho * c_{ij}^2$, respectively. ρ is the apparent or bulk density of the material, E_i is the modulus of elasticity in the i -direction, and G_{ij} is the shear modulus relating the strain $2e_{ij}$ to the stress T_{ij} . For these relationships to hold, the wavelength has to be larger than the characteristic dimensions of the specimen [16].

The measurement of the elastic constants is, however, a non-trivial task, independently of the methodology used. A preferred trabecular orientation (i.e. material symmetry) is often present, yet in many cases it is hardly recognizable. Turner and Cowin studied the errors caused by the misalignment between the measurement axes and the material symmetry axes in bone [14]. The authors found a mean error in the measured Young's moduli of 9.5% in cancellous bone when the misalignment angle was 10 degrees. This suggests that a significant part of the variability of the published elasticity values is associated with systematic errors in the measurements rather than with significant differences in material properties.

3.2. Indirect assessment of cancellous bone properties from large-scale finite element (FE) models

In the last decade, benchtop computer tomography (CT) systems have been developed that achieve a spatial resolution of 30 μm and better. These devices allow the reconstruction of the trabecular architecture inside cancellous bone samples at great detail and in three dimensions. By automated voxel conversion large-scale finite element (FE) models of the bone specimen can be created. These FE models can be used to calculate the elastic constants of cancellous bone by simulating mechanical testing protocols on the computer reconstructed specimen [17]. Homogeneous and isotropic tissue elastic properties are usually used as input to describe the elasticity of a single FE. This ultimately limits the investigation of bone elastic behavior to structural effects [18, 19]. The accuracy of the FE calculations is directly dependent on the convergence tolerance of the iterative algorithm used in the FE calculations. If the tolerance and the element dimensions are properly chosen, an accuracy of 1% can be achieved [17]. Additionally, if real mechanical tests are performed in conjunction with FE analysis, a comparison (scaling)

between experimental and computed values will provide an indirect estimate of the mean elastic modulus of the trabecular material. Using this approach, Hou and collaborators [20] calculated a mean trabecular tissue stiffness of 5.7 GPa (SD = 1.6 GPa, $n = 28$), whereas Ladd *et al.* [21] computed a mean value of 6.6 GPa (SD = 1.1 GPa, $n = 5$).

Recently, Jacobs [22] examined the accuracy of this approach using porous bone-like model systems made of polymethylmethacrylate (bone cement), a material with known mechanical properties. He concluded that the relative accuracy of the estimated elastic modulus is 2.2% when using an element size of 50 μm and as good as 0.5% when using an element size of 25 μm . This suggests that it is, in principle, possible to perform macroscopic mechanical tests and then to deduce the material properties from FE modeling using structural information based on micro-CT reconstructions. However, the validity of this approach still awaits a proof on real biological tissues, where the structural and material properties are known with less confidence.

4. Mechanical properties of single trabeculae and trabecular material

Assuming the existence of a preferred lamellar orientation along the trabecular longitudinal direction, trabecular bone tissue should be considered as transverse isotropic. Since trabeculae are supposedly loaded in bending and in tension/compression, the determination of the elastic modulus in the direction of the trabecular axis (in the following termed E_{trab}) may suffice to describe the bone elastic behavior. Numerous measurements of E_{trab} have been reported. They involve a variety of mechanical testing protocols such as tensile, three-point bending, four-point bending, and buckling of isolated trabeculae. Table I summarizes the results and relates them to the type of experimental protocol used. Most of these experiments were performed on single excised but unmachined trabeculae. The major problem encountered is the small size of the samples and, in the case of unmachined trabeculae, the complex geometry of the specimens (Fig. 1). The specific technical problems in performing mechanical tests on micrometer-size specimens will be discussed in Section 5. In the following, we briefly review the contributions listed in Table I. We contrast them in Table II to the values for the elastic modulus of

TABLE I Measured values for the elastic modulus of single unmachined trabeculae and of trabecular material

Authors	Exp. Protocol	Elastic Modulus	Further Information
Runkle, Pugh [24]	buckling	8.7 GPa (SD = 3.2 GPa)	—
Townsend <i>et al.</i> [25]	buckling	14.1 GPa	dry human bone ($n = 9$)
Townsend <i>et al.</i> [25]	buckling	11.4 GPa	wet human bone ($n = 9$)
Ashman, Rho [31]	ultrasound	13.0 GPa (SD = 1.47 GPa)	human bone ($n = 53$)
Ashman, Rho [31]	ultrasound	10.9 GPa (SD = 1.57 GPa)	bovine bone ($n = 15$)
Rho <i>et al.</i> [32]	tensile test	10.4 GPa (SD = 3.5 GPa)	dry human bone ($n = 20$)
Rho <i>et al.</i> [32]	ultrasound	14.8 GPa (SD = 1.4 GPa)	wet human bone ($n = 20$)
Mente, Lewis [26]	cantilever bending	6.2 GPa (SD = 1.8 GPa)	human bone ($n = 9$)
Ryan, Williams [27]	tensile test	0.76 GPa (SD = 0.39 GPa)	bovine bone ($n = 38$)
Kuhn <i>et al.</i> [28]	3-point bending	4.16 GPa (SD = 2.02 GPa)	human bone, old ($n = 29$)
Kuhn <i>et al.</i> [28]	3-point bending	3.03 GPa (SD = 1.63 GPa)	human bone, young ($n = 13$)
Choi <i>et al.</i> [29]	3-point bending	4.59 GPa (SD = 1.60 GPa)	human bone, old ($n = 20$)

TABLE II Elastic modulus of cortical bone as measured using machined specimens having similar dimensions as trabeculae

Authors	Exp. Protocol	Elastic Modulus	Further Information
Kuhn <i>et al.</i> [28]	3-point bending	5.26 GPa (SD = 2.09 GPa)	human bone, old ($n = 36$)
Kuhn <i>et al.</i> [28]	3-point bending	3.76 GPa (SD = 1.68 GPa)	human bone, young ($n = 12$)
Choi <i>et al.</i> [29]	3-point bending	5.44 GPa (SD = 1.25 GPa)	human bone, old ($n = 17$)
Rho <i>et al.</i> [32]	tensile test	18.6 GPa (SD = 3.5 GPa)	dry human bone ($n = 20$)
Rho <i>et al.</i> [32]	ultrasound	20.7 GPa (SD = 3.5 GPa)	wet human bone ($n = 20$)

micrometer-sized cortical bone samples. This allows a direct comparison of the two bone types on the microscopic scale.

In 1973, Pugh suggested that buckling of single trabeculae might be an important deformation mode in cancellous bone [23]. Runkle and Pugh [24] and Townsend [25] were the first investigators who attempted to calculate the elastic modulus of excised trabeculae from the measured buckling load. The mean modulus was 8.69 GPa (SD = 3.17 GPa) and 11.4 GPa (wet human bone), respectively.

Mente and Lewis [26] prepared cantilever specimens by potting single trabeculae taken from the femur and the tibia of unknown human donors. The trabeculae were mounted vertically to a translation stage, which was moved in x -direction towards a fixed loading head mounted parallel to the stage (cantilever bending test). A FE model of the examined trabeculae was generated to account for their bizarre geometries. The authors tuned the elastic modulus of the trabecular material in their FE model until they obtained a good match between the FE predicted and the experimentally observed load-deflection curve. The estimated mean E_{trab} was 5.3 GPa (SD = 2.6 GPa).

Tensile tests on trabeculae from bovine bone were performed by Ryan and Williams [27]. They determined the cross-sectional area using a hemacytometer grid, a device used in microscopy to count cells in a cell suspension. Because of the large variability in the collected data, we suspect that this approach provided only a rough estimate of the true value. The measured average E_{trab} was less than 1 GPa.

Goldstein and collaborators attempted to improve the experimental results and designed a micro-bending machine [28]. The loading device consisted of a microscope stage equipped with a load cell and a fixed, 160 μm wide loading head. The displacement was controlled using a stepper motor connected to the fine focus adjustment screw of the microscope. Given the difficulty in assessing the exact geometry of a whole trabecula, a special milling technique was used to machine specimens with a regular shape. The authors claimed that the milling procedure did not produce any tissue damage. Specimens from one 23-years-old donor and from one 63-years-old donor, both from cortical and trabecular bone, were machined to an average length of 1.5 mm, whereas base and height ranged from 50 μm to 200 μm . Both cancellous and cortical bone from the older donor were significantly stiffer (63-years old: $E_{\text{trab}} = 4.2$ GPa, $E_{\text{cort}} = 5.3$ GPa; 23-years old: $E_{\text{trab}} = 3.03$ GPa, $E_{\text{cort}} = 3.83$ GPa). These results suggest that, in agreement with Wolff's hypothesis, trabecular and cortical bone material are very similar in

terms of their elastic behavior. Later, Choi *et al.* repeated the measurements on micrometer-sized preparations of cortical and cancellous bone material taken from one single donor (human tibia, 60 years old) [29]. The experimental protocol was extended to investigate cortical bone specimens of different sizes (both height and base length varied between 100 μm and 1 mm). Interestingly, the elastic modulus increased from a value of 5 GPa to a value of 15 GPa with increasing specimen size. These observations were explained in terms of an increased impact of biological defects (such as lacunae) in smaller specimens, as postulated earlier by Rice *et al.* [30].

To overcome some of the technical difficulties of micromechanical testing, ultrasound measurements at high frequencies have been performed [31]. Ultrasound has the advantage to be a technique that is tunable to the dimensional requirements. To propagate sound waves along trabeculae, the frequency needs to be higher than currently used for waves propagating through macrosamples. Since the wavelength exceeds the dimensions of the tested volume, in this case a single trabecula, the density ρ can be considered as a constant (average density of the bone material over the trabecula). Ashman and Rho [31] obtained a value for E_{trab} of 13 GPa for human bone and of 11 GPa for bovine bone (no information about age and location). Rho and coworkers measured the elastic modulus of trabeculae taken from human tibiae (age unknown) both by ultrasound and tensile testing [32]. They found a mean E_{trab} of 10.4 GPa (SD = 3.5 GPa) from the tensile tests and of 14.8 GPa (SD = 1.4 GPa) from ultrasound wave propagation. In an additional experiment, micrometer-sized specimens of cortical bone from the same donors were tested. The average elastic modulus of the cortical material E_{cort} was 18.6 GPa (SD = 3.5 GPa) from the tensile tests and 20.7 GPa (SD = 1.9 GPa) from ultrasound measurements, respectively. Note that the results from tensile testing and ultrasound measurements cannot be directly compared because of the completely different strain rates involved in the two procedures. The values from the tensile test were significantly lower than the corresponding values obtained from ultrasound measurements, as expected from viscoelastic theory. However, it is interesting to note that cortical bone is significantly stiffer than trabecular bone, independently of the used testing procedure. The values of E_{cort} were shown to fall outside the 95% confidence intervals for E_{trab} . A multiple regression analysis correlating the elastic modulus to bone density showed that cortical bone is not simply dense cancellous bone as postulated by Wolff. Note that these results also contradict the findings from the Goldstein group [28, 29].

It seems that the mechanical resemblance between cortical and cancellous bone can be neither confirmed nor disproved with the currently known testing procedures. Prerequisite for a proof of Wolff's hypothesis is enhanced measurement accuracy. The uncertainties of existing procedures tend to mask any variation significant in terms of material behavior.

5. Error sources in micromechanical testing

The mechanical testing of a microsample necessarily leads to a downscaling of conventional procedures used for macroscopic structures. However, a one-to-one downscaling often fails because the expected forces and displacements in the microscopic domain cannot be resolved by measurement principles applicable in the macroscopic domain. The rapid progress in micro- and nanotechnology over the past decades has offered a completely new toolbox to biomechanics researchers experimenting with microscopic tissue samples. There is a broad variety of commercially available instruments for sensing and manipulation tasks at the microscopic scale. It remains now to the biomechanics community to combine these tools such that old and new questions of bone mechanics can be addressed with new efficiency.

With the advent of new instruments, there is always the challenge of mastering the novel data and to become able to derive meaningful conclusions. There is a number of fundamental issues which have to be addressed when interpreting results from micromechanical tests. First, the validity of the continuum model for the material under investigation has to be proved. Second, the effect of the increased surface-to-volume ratio in micrometer scale specimens as compared to regular ones, and consequently the increased importance of defects, must be taken into account. Third, the smaller the sample, the more the interactions between sample and instrument influence the experimental results. Before drawing any biomechanical conclusions, all possible error sources in the measurement need to be identified. Pure measurement artifacts have to be eliminated before data analysis. Finally, a proper investigation of the precision and accuracy has to be reported with every experiment in order to make the results comparable and quantitative.

5.1. General remarks on precision and accuracy

Precision is related to the experimental variation of a specific method in the determination of a target quantity. It depends only on the instrument and does not include the variability in sample response. Therefore, the precision of a method cannot be determined by repetitive measurements but needs to be derived from either theoretical considerations or dedicated calibration procedures. Accuracy, in contrast, describes the ability of a method to measure the true (but unknown) value of the target property. The factors which determine accuracy are related to both the testing method and the specimen. Before specifying accuracy, all the components of the measurement apparatus as well as the sample characteristics have to be examined. The smaller the scale, the more difficult it is to separate useful informa-

tion from artifacts in the testing device. For example, in micro-compression experiments, the load cell can deform to a degree similar to the specimen. Thus, an error is introduced when calculating strain from observing the total displacement of the actuator. Whenever possible, indirect measurement should be avoided. In the compression test, a direct optical observation of the strain would be much more appropriate. To our knowledge, this has been pursued for macroscopic testing of bone [33, 34], but not on the microscopic scale. On the other hand, the preparation (machining) and handling of the specimens will also affect the measurements. Specifically, in the case of micrometer-sized bone specimens and bone trabeculae, proper storage, controlled moisture conditions, and temperature control are some of the factors that will influence accuracy.

5.2. Error sources in tensile tests

Specimens of well-defined geometry are fixed in the grips of a tensile machine and force and elongation are independently monitored during the test. The elongation is usually not measured directly but derived from the actuator's displacement. The tensile test bears general advantages over other mechanical tests such as bending. From the load-elongation curve and the exact cross-sectional area, the characterization of a nearly uni-axial stress field is fairly simple. Additionally, the elastic modulus is linear in both the beam length and cross-sectional area, whereas in bending the elastic modulus is linear in the beam deflection, is proportional to the third power of beam length, and is quadratic in the cross-sectional area. Uncertainties in the reconstruction of the sample geometry have a worse impact on the results from bending tests than from tensile tests. However, there are two main sources of errors in tensile tests which arise particularly with the downscaling of the specimen. The first problem is related to sample fixation. Since gripping of single trabeculae is a difficult task, the specimens are usually glued into holes drilled in custom made grips. In most cases the bone deformation is simply set to the applied actuator displacement. The accuracy in estimating bone elasticity critically depends on a proper compensation of the glue deformation. However, to discriminate between bone deformation and glue deformation is difficult. The second problem is the sample alignment before and during the test. A proper alignment of the beam with the load axis is imperative to avoid uncontrolled shear stresses. In an inhomogeneous material such as bone, shear stresses will additionally originate from the different elastic behavior in different regions of the specimen as well as because of the irregular sample geometry. For a proper elasticity analysis, both factors have to be compensated based on measurements of the lamellar structure.

5.3. Error sources in bending tests

The bending test has advantages in terms of ease in practical implementation and of being insensitive to specimen misalignment. However, in a bending test stresses and strains are difficult to estimate. The application of the simple bending theory of a rod is valid

in the case of a homogeneous and isotropic material. For trabeculae, we expect a non-linear stress distribution due to a shift of the neutral axis. The deformations in tension and in compression do not obey the same laws. Additionally, inter-lamellar shear stresses will arise because of the layered composite nature of bone tissue. Finally, defects inside the specimen such as osteocyte lacunae will have local stress concentration effects.

The accuracy of the bending test depends mainly on the accuracy of the measurement of the geometric properties, in particular of the area moment of inertia. Taken a column with a radius R as an idealized model of a trabecula, the area moment of inertia I will be proportional to R^4 . Consequently, relative errors in the measurement of the radius propagate to four times larger relative errors in the area moment of inertia. The other factors determining the accuracy of elastic modulus estimates from bending tests can be derived from the simple equation (valid for a homogeneous and isotropic material in the linear range of the stress-strain relationship):

$$E = c * F * L^3 / I * d$$

The parameter c takes values dependent on the boundary conditions at both ends of the column. The modulus E obeys a relationship linear in the applied force F and the deflection d , but goes with the third power of the trabecular length L . Again, an accurate measurement of L is mandatory, in order to avoid large relative errors in the computation of E .

6. Potential improvements of existing methodologies

The development of micro-CT combined with 3D structural reconstruction and analysis delivered a precise picture of cancellous bone mechanics at the macroscopic level. In the near future this approach will further be enhanced in precision and resolution if the novel x-ray sources based on synchrotron radiation [35] are combined with state-of-the-art computational procedures.

The next step is the mechanical description of single trabeculae. In analogy to the characterization of bone mechanics on the macroscopic scale, trabecular mechanics can only be understood after an accurate reconstruction of the underlying architecture, i.e. the lamellar structure. The mechanical testing of trabeculae without a structural analysis will not fill the present gap of knowledge of the material bone on the microscopic scale. Structural models in conjunction with a reduction of experimental errors in the micro-mechanical testing could provide the biomechanics community with the sought information.

In the following, we formulate a few suggestions in order to improve the testing procedures. This list is derived from a careful reading of the reviewed articles and from own pilot experiments on single trabeculae. We have located five major areas of potential improvement:

Sample preparation: In micro-mechanical tests, special care should be devoted to sample preparation in order to avoid microdamage. To date, preparation techniques for single trabeculae have not been yet thoroughly evaluated. It is important to examine every sample for microcracks and other damage.

To our knowledge, the only protocol suited for achieving this goal has been proposed by Burr and Hooser [36]. Only intact specimens should be forwarded to the actual testing procedure. With this precaution, preparation-induced variability of the results may be minimized.

Measurement of the sample geometry: As analyzed in Sec. 5, the surface geometry of the sample trabecula has to be determined with high precision. A relative error of 10% in the radius specification of a column-like trabecula is amplified to 40% error in the elastic modulus if measured by means of bending tests. Using state of the art light microscopy it should be possible to measure the 3D topography of a trabecula with 1% precision. Given sample reconstruction, mathematical models are needed in order to compensate for the effect of topographic deviations from a regularly shaped standard (e.g. a column) in the final estimate of the stiffness matrix.

Analysis of boundary conditions: The boundary conditions (gripping, holding, and load application) have a great impact on the results. Protocols for an optimal alignment of the testing apparatus must be established. All the mechanically relevant components have to be calibrated before application. For instance, when applying glues for sample actuator connection, the elasticity of the glue has to be specified and documented in separate experiments.

Direct measurement of the dynamic quantities: Deformations and displacements should be measured directly on the sample. Optical methods, in particular the light microscope, which provides a view of the sample in real-time, have proven as appropriate tools for the quantification of sample dynamics in both bending and tensile tests [37, 38]. Ultimately, one should aim at a direct visualization and analysis of the strain field. This concept has been tested successfully on micro-rods [38]. Using a light microscope, there may be some concern regarding the diffraction limited resolution of the instrument. Assuming an elastic modulus of 10 GPa, the expected deflection of an ideal, beam-like trabecula (1 mm length, 100 μm radius) subjected to three-point bending amounts to about 1 μm . This number seems to be just in the range of the classic resolution of a light microscope equipped with dry objective lenses. However, we have experimentally and theoretically demonstrated that this resolution is not relevant for the detection of changes in position and shape of a specimen [39]. Using dry objectives and appropriate image processing software it was possible to measure deformations of micro-rods with a resolution of a few tens of nanometers [39]. The essential issue in duplicating these results on micrometer-sized bone specimens will be the generation of reliable image contrast. Conventional brightfield reflection or transmission microscopy are bound to fail due to the optical transparency of single trabeculae in the visible spectrum. Alternatively, we can exploit other contrast generating effects such as the well described autofluorescence of bone [40–42], artificial fluorescence labelling, or the natural birefringence of the collagen.

Structural analysis of the underlying lamellar architecture: Among all the requirements for an improvement of micromechanical tests, the structural analysis of the lamellar architecture is certainly the most challenging. Again, we speculate that the rapid progress in the development of new light microscopes will provide the key to this task. Compared to the electron microscope, light microscopy has the advantage of being minimal invasive in observation. Also, an integration of actuators for mechanical loading into the optical system is much easier with a light microscope than with an electron microscope.

A light microscope can be considered as a very versatile scattering machine in the spectrum between near ultraviolet and near infrared. The signal collected from a light microscope contains rich information about the material. It is encoded by the light-matter interaction, which takes place in either a transmission or a reflection path of light. It remains the task of the biomechanics community to make full use of the techniques provided nowadays by the microscopists. Furthermore, we can count on a constant extension of the toolbox, as other research communities put a lot of pressure on the further development of light microscopy. Especially attractive is the advent of multi-photon fluorescence excitation [43], fluorescence polarization [44], and 3D birefringence imaging. All these techniques have sufficient resolution to detect single lamellae and they have the potential to visualize the orientational inhomogeneity between the lamellar layers.

7. Summary

We reviewed past and current efforts undertaken to accurately assess the elasticity of cancellous bone, particularly at the microstructural level. We recognized several issues as critical for experimental success such as sample preparation and mounting, load application, and measurement of deformation. Accordingly, the interpretation of the published work is rather troublesome. The difficulty in evaluating the experimental results is manifested by the large variation in the values of E_{trab} .

Experimental data provide the necessary basis for an understanding of cancellous bone biomechanical behavior. In this paper, we formulated the need for a better and appropriate consideration of the bone microstructure and for a direct measurement of the strain field. We believe that the appropriate tools to achieve these goals either have already been made available or will be available in the near future.

References

1. R. P. HEANEY, *Calcif. Tissue Int.* **53**(Suppl 1) (1993) S3-6.
2. J. WOLFF, *Das Gesetz der Transformation der Knochen* August Hirschwald, Berlin, 1892.
3. G. H. BOURNE, "The Biochemistry and Physiology of Bone," vol. 1 (Academic Press, New York and London, 1972).
4. A. P. SPENCE, "Basic Human Anatomy" (The Benjamin/Cummings Publishing Company, Inc., Redwood City, CA 94065, 1990).
5. V. CANE, G. MAROTTI, G. VOLPI, D. ZAFFE, S. PALAZZINI, F. REMAGGI and M. A. MUGLIA, *Calcif. Tissue Int.* **34** (1982) 558.

6. W. J. WHITEHOUSE, *J. Microsc.* **101** (1974) 153.
7. T. P. HARRIGAN and R. W. MANN, *J. Mater. Sci.* **19** (1984) 761.
8. J. KRAGSTRUP, F. MELSEN and L. MOSEKILDE, *Metab-Bone-Dis-Relat-Res.* **4** (1983) 291.
9. F. LINDE, P. NORGAARD, I. HVID, A. ODGAARD and K. SOBALLE, *J. Biomech.* **24** (1991) 803.
10. S. C. COWIN, "Bone Mechanics" (CRC Press, Boca Raton, Fla., 1989).
11. S. C. COWIN and M. M. MEHRABADI, *J. Biomech.* **22** (1989) 503.
12. S. A. GOLDSTEIN, *ibid.* **20** (1987) 1055.
13. T. P. HARRIGAN, J. MURALI, R. W. MANN and W. H. HARRIS, *ibid.* **21** (1988) 269.
14. C. H. TURNER and S. C. COWIN, *J. Biomech. Eng.* **110** (1988) 213.
15. R. B. ASHMAN, J. D. CORIN and C. H. TURNER, *J. Biomech.* **20** (1987) 979.
16. R. B. ASHMAN, S. C. COWIN, W. C. VAN BUSKIRK and J. C. RICE, *ibid.* **17** (1984) 349.
17. B. VAN RIETBERGEN, H. WEINANS, R. HUISKES and A. ODGAARD, *ibid.* **28** (1995) 69.
18. B. VAN RIETBERGEN, A. ODGAARD, J. KABEL and R. HUISKES, *J. Orthop. Res.* **16** (1998) 23.
19. J. KABEL, B. VAN RIETBERGEN, M. DALSTRA, A. ODGAARD and R. HUISKES, *J. Biomech.* **32** (1999) 673.
20. F. J. HOU, S. M. LANG, S. J. HOSHAW, D. A. REIMANN and D. P. FYHRIE, *ibid.* **31** (1998) 1009.
21. A. J. C. LADD, J. H. KINNEY, D. L. HAUPT and S. A. GOLDSTEIN, *J. Orthop. Res.* **16** (1998) 622.
22. C. R. JACOBS, B. R. DAVIS, C. J. RIEGER, J. J. FRANCIS, M. SAAD and D. P. FYHRIE, *J. Biomech.* **32** (1999) 1159.
23. J. W. PUGH, *Bull. Hosp. Joint Dis.* **34** (1973) 92.
24. J. C. RUNKLE and J. W. PUGH, *ibid.* **36** (1975) 2.
25. P. R. TOWNSEND, R. M. ROSE and E. L. RADIN, *J. Biomech.* **8** (1975) 199.
26. P. L. MENTE and J. L. LEWIS, *J. Orthop. Res.* **7** (1989) 456.
27. S. D. RYAN and J. L. WILLIAMS, *J. Biomech.* **22** (1989) 351.
28. J. L. KUHN, S. A. GOLDSTEIN, K. CHOI, M. LONDON, L. A. FELDKAMP and L. S. MATTHEWS, *J. Orthop. Res.* **7** (1989) 876.
29. K. CHOI, J. L. KUHN, M. J. CIARELLI and S. A. GOLDSTEIN, *J. Biomech.* **23** (1990) 1103.
30. J. C. RICE, S. C. COWIN and J. A. BOWMAN, *ibid.* **21** (1988) 155.
31. R. B. ASHMAN and J. Y. RHO, *ibid.* **21** (1988) 177.
32. J. Y. RHO, R. B. ASHMAN and C. H. TURNER, *ibid.* **26** (1993) 111.
33. A. ODGAARD, I. HVID and F. LINDE, *ibid.* **22** (1989) 829.
34. A. ODGAARD and F. LINDE, *ibid.* **24** (1991) 691.
35. M. SALOME, F. PEYRIN, P. CLOETENS, C. ODET, A. M. LAVAL-JEANTET, J. BARUCHEL and P. SPANNE, *Med. Phys.* **26** (1999) 2194.
36. D. B. BURR and M. HOOSER, *Bone* **17** (1995) 431.
37. G. DANUSER, P. T. TRAN and E. D. SALMON, *J. Microsc.* **198** (2000) 34.
38. E. MAZZA, G. DANUSER and J. DUAL, *Microsystem Technologies* **2** (1996) 83.
39. G. DANUSER and E. MAZZA, In "Optical Inspection and Micromasurements," edited by C. Gorecki, vol. 2782 (European Optical Society, SPIE, 1996) p. 180.
40. A. I. D. PRENTICE, *Nature* **206** (1965) 1167.
41. C. H. BACHMAN and E. H. ELLIS, *ibid.* **206** (1965) 1328.
42. A. I. D. PRENTICE, *J. Clin. Path.* **20** (1967) 717.
43. W. DENK, J. H. STRICKLER and W. W. WEBB, *Science* **248** (1990) 73.
44. T. FUNATSU, Y. HARADA, M. TOKUNAGA, K. SAITO and T. YANAGIDA, *Nature* **374** (1995) 555.

Received 20 December 1999
and accepted 15 May 2000